SCIENCE CHINA
Life Sciences

•LETTER TO THE EDITOR•

March 2023 Vol.66 No.3: 639–642
https://doi.org/10.1007/s11427-022-2192-5

Cross-species binding spectrum of ACE2 to SARS-CoV-2 RBD

Xihao Liao[1†], Changge Guan[1†], Chenghua Wang[2†], Xinjie Chen[1†], Xiaomei Lin[1], Lianghua Lu[2], Lu Li[1], Ting Wang[1], Nan Su[1], Bian Wu[3], Xinquan Wang[4], Chong Zhang[1,5], Yi Wang[1*], Yuan Lu[1*] & Xin-Hui Xing[1,5,6,7*]

[1]*Key Laboratory for Industrial Biocatalysis, Ministry of Education of China, Department of Chemical Engineering, Tsinghua University, Beijing 100084, China;*
[2]*College of Light Industry and Food Engineering, Guangxi University, Nanning 530004, China;*
[3]*CAS Key Laboratory of Microbial Physiological and Metabolic Engineering, State Key Laboratory of Microbial Resources, Institute of Microbiology, Chinese Academy of Sciences, Beijing 100101, China;*
[4]*The Ministry of Education Key Laboratory of Protein Science, Beijing Advanced Innovation Center for Structural Biology, Beijing Frontier Research Center for Biological Structure, Collaborative Innovation Center for Biotherapy, School of Life Sciences, Tsinghua University, Beijing 100084, China;*
[5]*Center for Synthetic and Systems Biology, Tsinghua University, Beijing 100084, China;*
[6]*Institute of Biopharmaceutical and Health Engineering, Tsinghua Shenzhen International Graduate School, Shenzhen 518055, China;*
[7]*Institute of Biomedical Health Technology and Engineering, Shenzhen Bay Laboratory, Shenzhen 440300, China*

Received July 14, 2022; accepted September 3, 2022; published online November 29, 2022

Citation: Liao, X., Guan, C., Wang, C., Chen, X., Lin, X., Lu, L., Li, L., Wang, T., Su, N., Wu, B., et al. (2023). Cross-species binding spectrum of ACE2 to SARS-CoV-2 RBD. Sci China Life Sci 66, 639–642. https://doi.org/10.1007/s11427-022-2192-5

Dear Editor,

Severe acute respiratory syndrome coronavirus 2 (SARS-CoV-2) is the cause of COVID-19, which has posed a massive threat to human health, economy, and security worldwide (Bai et al., 2022). Genomic analysis of SARS-CoV-2 and related coronaviruses revealed that SARS-CoV and SARS-CoV-2 likely had ancestors (Xu et al., 2020), which might originate in bats, followed by subsequent spread within intermediate hosts (spillover hosts) and then transmission to humans (Wang et al., 2021). The host range of both viruses may be expanded to include primates and other mammals (Liu et al., 2021). Angiotensin-converting enzyme 2 (ACE2) has been proved as the main responsible receptor for SARS-CoV-2 to infect human cells by specifically interacting with the receptor-binding domain (RBD) of spike (S) protein in (Lan et al., 2020). Consequently, characterizing the interaction between SARS-CoV-2 S and ACE2 orthologs from various species is crucial for pursuing the intermediate host candidates. Recently, functional analysis of ACE2 orthologs revealed that pets, domestic animals, and multiple wild animals could bind to SARS-CoV-2 RBD and promote the pseudovirus transduction (Wu et al., 2020). However, current recombinant ACE2 expression relies on insect and mammalian cells with low yield (<1 mg L^{-1}) and long production cycle (Zhang et al., 2020).

Here, we propose developing microbial cells to express ACE2 homologs to analyze the cross-species evolution features of ACE2 receptors binding with SARS-CoV-2 RBD. We performed a phylogenetic analysis of 31 vertebrate species covering domestic and wild animals from 13 orders in four vertebrate classes (mammals, amphibians, reptiles, and fishes) (Figure 1A and Table S1 in Supporting Information). 16 key residues in human ACE2 (hACE2) responsible for the interaction with RBD were highlighted (Lan et al., 2020). We compared these residues of 31 ACE2 orthologs with hACE2 and found more substitutions were observed in amphibians, reptiles, and fishes by contrast to

†Contributed equally to this work
*Corresponding authors (Yi Wang, email: wangyi671@mail.tsinghua.edu.cn; Yuan Lu, email: yuanlu@tsinghua.edu.cn; Xin-Hui Xing, email: xhxing@tsinghua.edu.cn)

mammals. The C-terminal region is more evolutionarily conserved than N-terminal and Middle regions. To verify evolution analysis results, ACE2s from 15 species were heterologously expressed, including marmot, tiger, cat, cattle, pig, and dog with fewer substitutions, mink, ferret, pangolin, rat, civet, bat, and zebrafish with middle substitutions, snake and turtle with more substitutions.

Full-length hACE2 (805 aa) consists of a signal peptide (1–17 aa), an ectodomain (18–740 aa), and a single transmembrane helix with a ~40-residue intracellular segment. hACE2 dimerizes through two interfaces, the PD and the neck domain (616–740 aa) (Yan et al., 2020). To investigate the effect of hACE2 structure on its binding to RBD, we expressed hACE2(18–615 aa) and hACE2(18–740 aa) in three hosts, respectively (Figures S1–S3 in Supporting Information). The results showed that they were successfully secreted in yeast *Pichia pastoris* (*P. pastoris*) (Figure 1D). The binding affinity of *P. pastoris* and HEK293 hACE2 (740) was similar (Figures S4 and S5 in Supporting Information, Figure 1D). Inclusion of the natural C-terminal ACE2 collectrin domain (residues 615 to 740) could improve the binding affinity (Figure 1D). The molecular weight analysis revealed that hACE2(740) was a dimer while hACE2(615) was a monomer (Figure 1D). Overall, these results demonstrated that hACE2 expressed by *P. pastoris* could effectively bind to SARS-CoV-2 RBD, and the length of hACE2 ectodomain affected interaction.

To study the interaction between SARS-CoV-2 RBD and ACE2 orthologs, ACE2(615/740)s of 15 animals were expressed in *P. pastoris* (Figures S6 and S7 in Supporting Information). For ACE2(615) orthologs, ELISA and BLI analysis showed binding affinities lower than hACE2(615) (Figure S8 and S9 in Supporting Information). ACE2(740) orthologs to SARS-CoV-2 RBD. While, ACE2(740) orthologs displayed significantly higher binding signals than ACE2(615)s (Figure 1B and Figure S10 in Supporting Information), suggesting that ACE2 protein length affected RBD binding affinities. Previous studies (Glasgow et al., 2020), as well as our results, demonstrated that the residues (615 to 740) contributing to hACE2 dimerization boosted the binding affinity (Figure 1D). However, only part of ACE2 (740) orthologs among different species were dimerized (Table S2), suggesting that ACE2 ortholog length, not dimerization, was crucial for the binding affinity. Thus, ACE2 (740) might better characterize RBD binding. By comparing the binding affinities of ACE2(740) orthologs with hACE2 (740) to RBD, pig and tiger were similar to human; marmot and cattle were 1.5–2 fold weaker; pangolin, dog, and cat were 3–6 fold weaker; mink, snake, and civet were 80–200 fold weaker; rat and turtle showed poor binding signals; ferret, bat, and zebrafish showed no binding. Interestingly, minks and ferrets are both from the same mammal family, and their appearances look very similar, but their binding affinities differ (Figure S9 in Supporting Information and Figure 1B). Previous studies showed that some rodentia ACE2s were not binding to RBD, such as mouse, rat, and Guinea pig (Liu et al., 2021; Wu et al., 2020); here, we demonstrated that marmot ACE2 could effectively bind to RBD as a possible intermediate host. Overall, reptile and fish ACE2 showed insignificant binding to RBD.

To determine whether the residue substitutions in ACE2 orthologs affect the binding to SARS-CoV-2 RBD, we analyzed the correlation between substitutions of 16 key residues and binding affinities (KD value) (Figure 1C and Figure S11 in Supporting Information). Then Y_i value was calculated by using the equation $Y_i=-\log_{10}KD_i$ (KD_i denotes KD value of i kind of animal), the substitution numbers of i kind of animal in three regions (N-terminal, Middle, C-terminal) were as x_i^1, x_i^2, x_i^3, and multiple linear regression was used to fit Y_i and x_i^j (j=1, 2, 3). We found that x_i^1 (P<0.05) was significantly related to KD value, while x_i^2 and x_i^3 were not related to KD value, suggesting that the N-terminal region was important for the binding between ACE2 and RBD. This result indicated that we should pay more attention to the residues in N-terminal region for evolutionary analysis of ACE2/RBD binding. Moreover, regression analysis on the total number of substitutions was found to be significantly correlated with the KD value. The results revealed that the binding affinities between ACE2 (740) orthologs and SARS-CoV-2 RBD were related to the substitutions of 16 residues on the interaction surface.

To understand the molecular basis of ACE2 orthologs binding to SARS-CoV-2 RBD, we constructed ACE2 models using AlphaFold 2 (Figure S12 in Supporting Information) and investigated protein-protein docking (Figures S13 and S14 in Supporting Information). The docking scores of turtle, dog, bat, rat, and zebrafish ACE2s with RBD were higher, indicating weaker affinities and more unstable complex structures, consistent with BLI results (Figure S9 and Table S3 in Supporting Information). Meanwhile, diversified interactions between ACE2 orthologs and RBD were observed (Figure S15 and Table S4 in Supporting Information). Cattle, cat, mink, and civet ACE2s possessed similar intermediate binding affinities (Figure S9 in Supporting Information), but marmot, pig, and pangolin ACE2s had higher binding affinities. More substitutions from N-terminal and middle regions of ACE2s occurred in amphibians, reptiles, and fishes compared with mammals (Figure 1A), thereby affecting the interaction state with RBD (Figure S15 in Supporting Information). In addition, structural variations in marmot, pig, and pangolin ACE2/RBD complexes affected docking (Figures S14 and S15 in Supporting Information). Taken together, these findings implied that the precise interactions between ACE2s and SARS-CoV-2 RBD were related to the key residue substitutions and their three-dimensional structures.

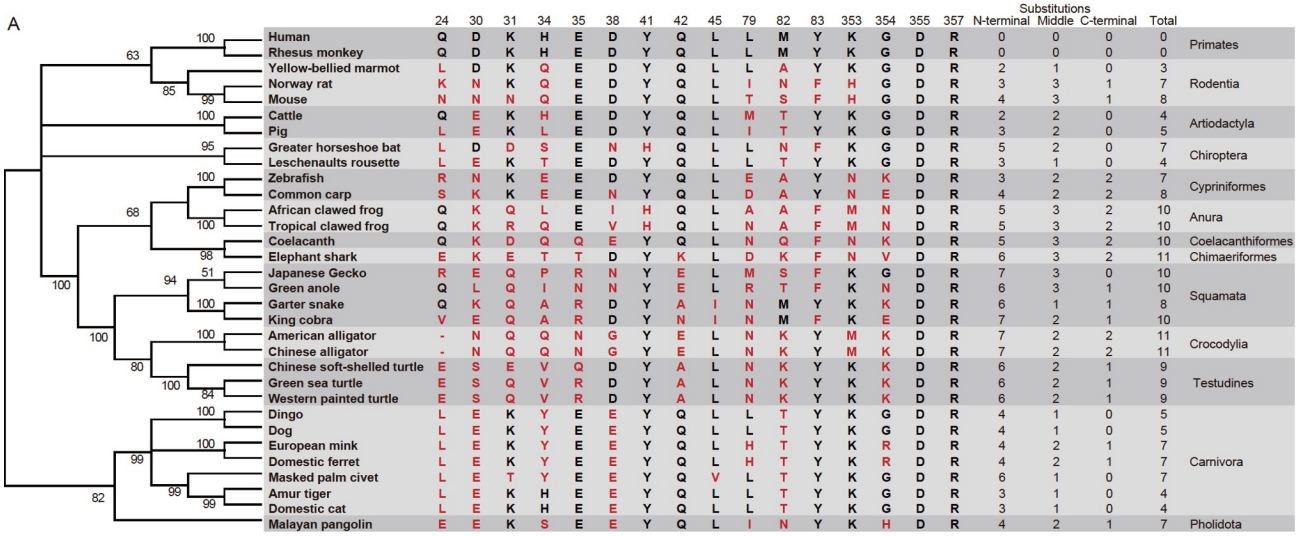
A
Substitutions
24 30 31 34 35 38 41 42 45 79 82 83 353 354 355 357 N-terminal Middle C-terminal Total
Human Q D K H E D Y Q L L M Y K G D R 0 0 0 0 Primates
Rhesus monkey Q D K H E D Y Q L L M Y K G D R 0 0 0 0
Yellow-bellied marmot L D K Q E D Y Q L L A Y K G D R 2 1 0 3 Rodentia
Norway rat K N K Q E D Y Q L I N F H G D R 3 3 1 7
Mouse N N N Q E D Y Q L T S F H G D R 4 3 1 8
Cattle Q E K H E D Y Q L M T Y K G D R 2 2 0 4 Artiodactyla
Pig L E K L E D Y Q L I T Y K G D R 3 2 0 5
Greater horseshoe bat L D D S E N H Q L L N F K G D R 5 2 0 7 Chiroptera
Leschenaults rousette L E K T E D Y Q L L T Y K G D R 3 1 0 4
Zebrafish R N K E E D Y Q L E A Y N K D R 3 2 2 7 Cypriniformes
Common carp S K K E E N Y Q L D A Y N E D R 4 2 2 8
African clawed frog Q K Q L E I H Q L A A F M N D R 5 3 2 10 Anura
Tropical clawed frog Q K R Q E V H Q L N A F M N D R 5 3 2 10
Coelacanth Q K D Q Q E Y Q L N Q F N K D R 5 3 2 10 Coelacanthiformes
Elephant shark E K E T T D Y K L D K F N V D R 6 3 2 11 Chimaeriformes
Japanese Gecko R E Q P R N Y E L M S F K G D R 7 3 0 10 Squamata
Green anole Q L Q I N N Y E L R T F K N D R 6 3 1 10
Garter snake Q K Q A R D Y A I N M Y K K D R 6 1 1 8
King cobra V E Q A R D Y N I N M F K E D R 7 2 1 10
American alligator - N Q Q N G Y E L N K Y M K D R 7 2 2 11 Crocodylia
Chinese alligator - N Q Q N G Y E L N K Y M K D R 7 2 2 11
Chinese soft-shelled turtle E S E V Q D Y A L N K Y K K D R 6 2 1 9 Testudines
Green sea turtle E S Q V R D Y A L N K Y K K D R 6 2 1 9
Western painted turtle E S Q V R D Y A L N K Y K K D R 6 2 1 9
Dingo L E K Y E E Y Q L L T Y K G D R 4 1 0 5 Carnivora
Dog L E K Y E E Y Q L L T Y K G D R 4 1 0 5
European mink L E K Y E E Y Q L H T Y K R D R 4 2 1 7
Domestic ferret L E K Y E E Y Q L H T Y K R D R 4 2 1 7
Masked palm civet L E T Y E E Y Q V L T Y K G D R 6 1 0 7
Amur tiger L E K H E E Y Q L L T Y K G D R 3 1 0 4
Domestic cat L E K H E E Y Q L L T Y K G D R 3 1 0 4
Malayan pangolin E E K S E E Y Q L I N Y K H D R 4 2 1 7 Pholidota
100 63 100 85 99 100 95 100 68 100 98 51 94 100 100 100 80 100 84 100 100 99 99 82 99
B
Human KD=9.59 nmol L⁻¹
Pig KD=7.18 nmol L⁻¹
Amur tiger KD=7.51 nmol L⁻¹
Yellow-bellied marmot KD=14.1 nmol L⁻¹
Cattle KD=17.5 nmol L⁻¹
Malayan pangolin KD=32 nmol L⁻¹
Dog KD=44 nmol L⁻¹
Domestic cat KD=55.2 nmol L⁻¹
European mink KD=0.801 μmol L⁻¹
Garter snake KD=1.06 μmol L⁻¹
Masked palm civet KD=1.85 μmol L⁻¹
Norway rat KD=24.8 μmol L⁻¹
Chinese soft-shelled turtle KD=387 μmol L⁻¹
Domestic ferret
Greater horseshoe bat
Zebrafish
Response (nm)
Time (s)
C
N-terminal
Middel
C-terminal
Total
Mutation number

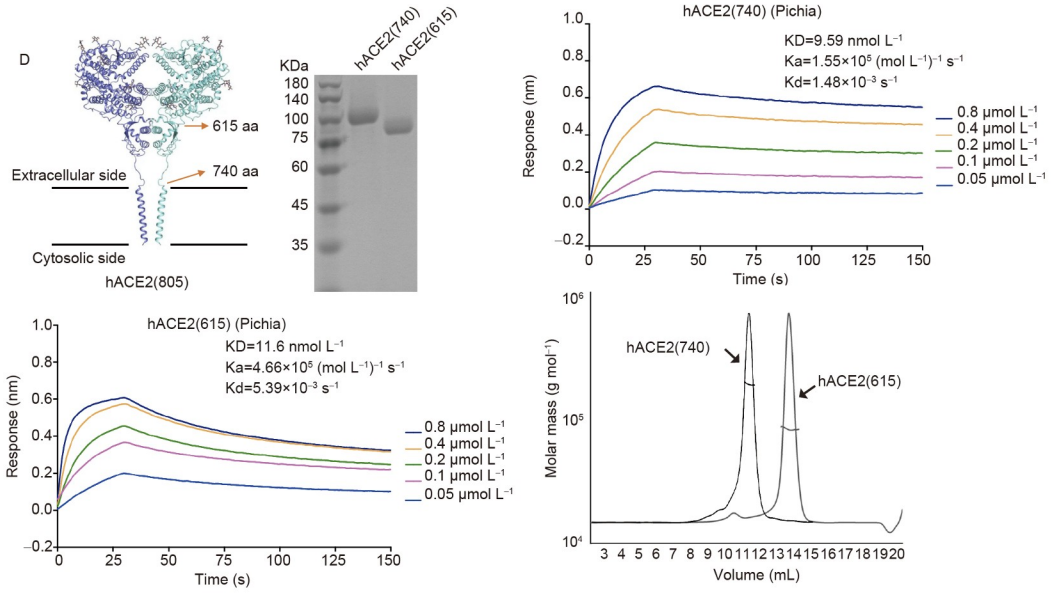

Figure 1 Cross-species evolution features of ACE2 receptors binding with SARS-CoV-2 RBD. A, Phylogenetic analysis of 31 species based on ACE2 and characteristics of the SARS-CoV-2 RBD-binding residues of ACE2s. Phylogenetic tree based on ACE2 amino acids sequence was generated using MEGA X. The 31 species belonging to 13 orders are shown in the right column. Sixteen key residues of hACE2 for interacting with SARS-CoV-2 RBD were listed. Red letters suggested the substitutions in the ACE2 of 31 species. B, The binding affinity of 16 ACE2(740) orthologs to SARS-CoV-2 RBD by BLI. C, Correlation analysis between the number of substitutions of 16 residues of ACE2 orthologs and KD values. D, Expression and characterization of hACE2 (740/615) in *P. pastoris*. SDS-PAGE analysis of hACE2(740/615) was performed after purification. BLI kinetics of hACE2(740/516) binding to immobilized RBD-mFc with association (t=0 to 30 s) and dissociation (t>120 s). Monomer and dimer for truncated hACE2 were confirmed by SEC. Y=−$\log_{10}$KD.

In conclusion, we have built a simple and quick platform for the *in vitro* characterization of SARS-CoV-2 S RBD/ACE2 interactions. This simple and low-cost platform allows us to manufacture ACE2 proteins in a small amount of time. According to the findings of this study, despite the rapid *in vitro* characterization of the ACE2/RBD interaction, more research on infection potential is required using cell cultures, stem cells, organoids, and other methods such as direct animal infection studies at the BSL-3 laboratory and SARS-CoV-2-specific antibody detections in wild animals.

Compliance and ethics *The author(s) declare that they have no conflict of interest.*

Acknowledgements *This work was supported by Tsinghua University Spring Breeze Fund (2020Z99CFZ023).*

References

Bai, C., Zhong, Q., and Gao, G.F. (2022). Overview of SARS-CoV-2 genome-encoded proteins. Sci China Life Sci 65, 280–294.

Glasgow, A., Glasgow, J., Limonta, D., Solomon, P., Lui, I., Zhang, Y., Nix, M.A., Rettko, N.J., Zha, S., Yamin, R., et al. (2020). Engineered ACE2 receptor traps potently neutralize SARS-CoV-2. Proc Natl Acad Sci USA 117, 28046–28055.

Lan, J., Ge, J., Yu, J., Shan, S., Zhou, H., Fan, S., Zhang, Q., Shi, X., Wang, Q., Zhang, L., et al. (2020). Structure of the SARS-CoV-2 spike receptor-binding domain bound to the ACE2 receptor. Nature 581, 215–220.

Liu, Y., Hu, G., Wang, Y., Ren, W., Zhao, X., Ji, F., Zhu, Y., Feng, F., Gong, M., Ju, X., et al. (2021). Functional and genetic analysis of viral receptor ACE2 orthologs reveals a broad potential host range of SARS-CoV-2. Proc Natl Acad Sci USA 118, e2025373118.

Wang, Q., Chen, H., Shi, Y., Hughes, A.C., Liu, W.J., Jiang, J., Gao, G.F., Xue, Y., and Tong, Y. (2021). Tracing the origins of SARS-CoV-2: lessons learned from the past. Cell Res 31, 1139–1141.

Wu, L., Chen, Q., Liu, K., Wang, J., Han, P., Zhang, Y., Hu, Y., Meng, Y., Pan, X., Qiao, C., et al. (2020). Broad host range of SARS-CoV-2 and the molecular basis for SARS-CoV-2 binding to cat ACE2. Cell Discov 6, 68.

Xu, X., Chen, P., Wang, J., Feng, J., Zhou, H., Li, X., Zhong, W., and Hao, P. (2020). Evolution of the novel coronavirus from the ongoing Wuhan outbreak and modeling of its spike protein for risk of human transmission. Sci China Life Sci 63, 457–460.

Yan, R., Zhang, Y., Li, Y., Xia, L., Guo, Y., and Zhou, Q. (2020). Structural basis for the recognition of SARS-CoV-2 by full-length human ACE2. Science 367, 1444–1448.

Zhang, H., Penninger, J.M., Li, Y., Zhong, N., and Slutsky, A.S. (2020). Angiotensin-converting enzyme 2 (ACE2) as a SARS-CoV-2 receptor: molecular mechanisms and potential therapeutic target. Intensive Care Med 46, 586–590.

SUPPORTING INFORMATION

The supporting information is available online at https://doi.org/10.1007/s11427-022-2192-5. The supporting materials are published as submitted, without typesetting or editing. The responsibility for scientific accuracy and content remains entirely with the authors.